Surfactant-Polymer Coreflood Simulation and Uncertainty Analysis Derived from Laboratory Study

Farizal Hakiki[1,2*], Dara Ayuda Maharsi[2] & Taufan Marhaendrajana[1,2]

[1]OGRINDO Research Consortium, Institut Teknologi Bandung,
Petrol. Eng. Bldg, Level 2, Jalan Ganesha No. 10, Bandung 40132, Indonesia
[2]Petroleum Engineering Study Program, Institut Teknologi Bandung,
Jalan Ganesha No. 10, Bandung 40132, Indonesia
[*]Email: alhakiki@alumni.itb.ac.id

Abstract. This paper presents a numerical simulation study on coreflood scale derived from a laboratory study conducted on light oil and water-wet sandstone samples from fields at Tempino and Kenali Asam, Sumatra, Indonesia. A rigorous laboratory study prompted a specified surfactant type among dozens of screened samples, i.e. AN3NS and AN2NS-M for Kenali Asam and Tempino, respectively. The coreflood scale numerical simulation study was performed using a commercial simulator, on the basis of the results from the laboratory study, at a constant temperature of 68°C, 0.3 cc/min injection rate and under 120 psia confining pressure. To get better recovery, the cores were tested using surfactant and polymer in a blended mode, containing 0.03% w/w polymer diluted in each field brine, which accommodated around 8000 ppm salinity. The most significant variable in the multiphase flow is the relative permeability curve, which is affected by interfacial tension (IFT) during waterflooding and surfactant-polymer (SP) flooding. This study shows that relative permeability will be shifted at ultra-low IFT (10^{-3} to 10^{-4} mN/m). This shifting phenomenon is governed by the interpolation parameter set, which implicitly represents the capillary number. Further work in matching the numerical results to the coreflood was conducted by changing the interpolation parameters.

Keywords: *blending surfactant-polymer; capillary number; coreflood matching; coreflood simulation; EOR history matching; relative permeability; ultra-low IFT; uncertainty analysis.*

1 Introduction

Enhanced oil recovery (EOR) screening, carried out based on Al-Adasani and Bai [1], revealed that the Tempino and Kenali Asam reservoirs are very suitable for polymer flooding; they were ranked in first place. Austad, *et al.* [2], followed by Samanta [3], have reported that significant improvements can be obtained by co-injecting surfactant and polymer at a rather low chemical concentration. Surfactant is a chemical compound comprising one hydrocarbon chain (lipophilic) and a polar head (hydrophilic). Surfactant is able to reduce the interfacial tension (IFT) between oil and water and to alter the wetting phase

Received March 7th, 2015, 1st Revision May 6th, 2015, 2nd Revision June 16th, 2015, 3rd Revision August 6th, 2015, 4th Revision September 10th, 2015, Accepted for publication October 8th, 2015.
 ISSN: 2337-5779, DOI: 10.5614/j.eng.technol.sci.2015.47.6.9

behavior. The lowering of tension in the water and oil interface is the main driving force that enables the use of chemical EOR [4]. Because of this characteristic the surfactant is considered to be an EOR agent. The use of surfactant-polymer gives more recovered oil than a surfactant injection only, due to the synergistic contribution of IFT reduction by the surfactant and mobility ratio reduction by the polymer [3,5]. A previous study on the effect of alkali on alkaline-surfactant-polymer (ASP) flooding showed that additional oil recovery could be obtained by increasing the concentration of alkali due to in-situ formation of surfactant [6]. Nevertheless, in the authors' laboratory experiments, the alkali affected the stability of the injected surfactant at a high temperature (70°C) to form aggregates that increased IFT. Therefore, this study does not include alkali in the chemical slug.

One of main purposes of chemical flooding is to reduce oil saturation, which is related to the capillary number [7]. The residual oil saturation will remain constant if the injection process is operated at a low capillary number ($N_C < 10^{-5}$), as happens in water flooding [8]. An increment of the capillary number will have the effect of lowering the residual oil saturation. A high capillary number can be achieved by reducing IFT.

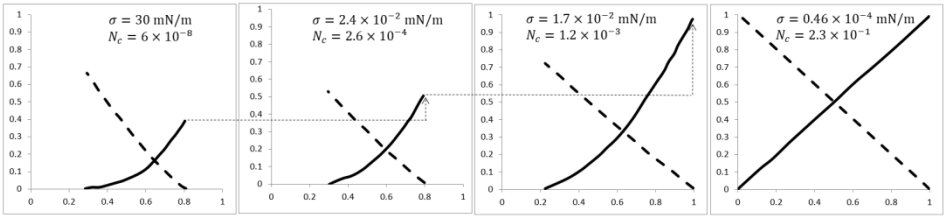

Figure 1 Relative permeability curve for oil-water and oil-micellar system. The bold and dash lines are water and oil relative permeability, respectively. Data digitised from Van Quy and Labrid [9].

It was found that the most representative parameter in multiphase flow under reservoir is the relative permeability curve (relperm curve) [10]. IFT reduction will alter the relative permeability and influences each phase flow behavior [10-14]. In a numerical study on chemical injection it was observed that the relative permeability curve can be represented by 4 curves that are obtained from measurements and show 2 extreme and 2 transition conditions (Figure 1) [9]. The extreme conditions show a displacement of oil by water and displacement of oil-water by micro-emulsions. The figures (left to right) show that reducing IFT will improve the relative permeability and alter its curvature while decreasing the residual oil saturation (S_{or}) and connate water saturation (S_{wc}). From 1st to 3rd sub-figures of Figure 1, the reduction of connate water saturation

is not really significant. In addition, Van Quy and Labrid [9] developed relative permeability curve correlations as a function of IFT.

Pope*, et al.* [15] emphasize that relative permeability curves should not be modeled based on IFT only but also include a trapping number, N_T. Their study showed that prediction of the relative permeability curve with respect to IFT can be done using information on the residual saturation, S_{lr}^{low}, and the end-point permeability, k_{rl}^{low}, at a low trapping number if the desaturation curve is known.

Other authors have developed a reservoir simulator that can govern Pope's study to express relative permeability alteration [16,17]. Some instances have been adopted in UTCHEM™ and CMG STARS™. CMG STARS™ includes the compositional effect on relative permeability. In this case, the ability to interpolate from the initial relative permeability curve and capillary pressure data as a function of concentration and capillary number was proven to be able to show the composition change in a reservoir. Another simulator uses the IFT effect with respect to relative permeability, which can be assessed based on the desaturation curve. CMG STARS™ uses the wetting phase interpolation parameter (*DTRAPW*) and the non-wetting phase interpolation parameter (*DTRAPN*) for obtaining an interpolated relative permeability between two relative permeability curves at high IFT (low N_C) and low IFT (high N_C) [18].

In this study a surfactant-polymer coreflood numerical study was performed using a commercial simulator, CMG STARS™. The study's objectives included assessment and determination of uncertain parameters related to relative permeability alteration that greatly affect the surfactant-polymer simulation results. Detailed parameters and steps are presented under Section 2 (Method).

It is important to note that permeability reduction may occur as a result of polymer adsorption by the rock surface, as pointed out by Mishra*, et al.* [19]. These permeability changes add complexity and uncertainty during surfactant-polymer injection. In this study, absolute permeability changes were not regarded since the polymer concentration was very small (0.03% or equivalent to 300 ppm). Therefore, this study focused on modeling the uncertainty of the relative permeability alteration due to the changes of the capillary number.

The four curves of Van Quy and Labrid [9], which were published by CMG in its *User's Guide* [18], can be presented in two ways. The first one uses the interpolation parameter *DTRAPW* and the following critical capillary numbers:

N_C = 6.0E−8 (either oil or water saturation is reduced),
N_C = 2.6E−4 (intermediate curve [9]),

N_C = 1.2E−3 (residual oil saturation reaches zero),
N_C = 2.3E−1 (irreducible water saturation reaches zero, relative permeability curve shows a straight line).

The next step is inputting two relative permeability curves using *DTRAPW* and *DTRAPN*, as follows:

1. High IFT (without surfactant), *DTRAPW* = *DTRAPN* = log(6.0E−8).
2. Ultra-low IFT (straight line), *DTRAPW* = log(2.3E−1) and *DTRAPN* = log(1.2E−3).

The three phases of the relative permeability curve and capillary pressure can be calculated based on interpolating data sets A and B (low and high N_C) using Eqs. (2), (3) and (4), which are presented in the Appendix.

2 Method

2.1 Materials

For the experimental work on the Kenali Asam cores, AN3NS was selected. This is a mixture of anionic ethoxy carboxylate derived from palm oil and non-ionic ethoxylate (Figure 2). The surfactant was then blended with 0.03% hydrolyzed polyacrylamide (HPAM) polymer, named F3630S and provided by SNF Florindo, with a mass concentration of 2% surfactant. Meanwhile, for the Tempino cores AN2NS-M was employed, another mixture of anionic ethoxy carboxylate derived from palm oil and non-ionic ethoxylate. Blended slug consisting of a surfactant solution of 1% w/w AN2NS-M and 0.03% w/w polymer F3630S. The surfactants were pre-screened from dozens of surfactant samples. The surfactant screening method followed Swadesi*, et al.* [20].

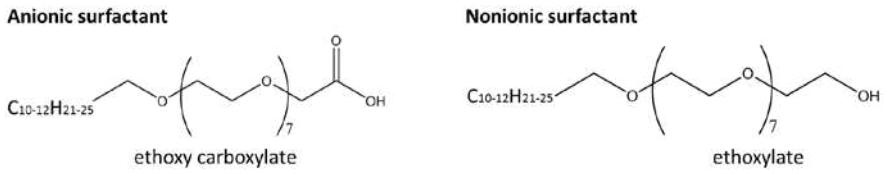

Figure 2 Molecular structure of surfactant AN3NS component.

2.2 Modeling

Numerical modeling was carried out using CMG STARS™ with the aim of validating the surfactant and rock-fluid model at ultra-low IFT and finding the history matching parameters that were used as input in the field-scale simulation. The matching parameters that were tested in this study are:

1. Phase interpolation parameters at low and high N_C (*DTRAPW* and *DTRAPN*)
2. End-point of relative permeability curve at low N_C
3. End-point and relative permeability curve profile at high N_C
4. Residual oil saturation at low and high N_C

The model that was built was a 1-D model with the producer and the injector well at the edge of the numerical grid. Field cores physically have cylindrical dimensions that are specified in diameter and length. In the numerical modeling using CMG STARS™, the model was built in Cartesian coordinates (*X, Y, Z*). When adjusting the numerical model to the real physical model it is vital to have the same numerical pore volume and oil phase volume. A comparison of the values for native core from the Kenali Asam field (KAS) and the Tempino field (TPN) are presented in Table 1. Hence, the Volume Modifier for Array Properties of CMG STARS™ was employed to gain the initial matching. The pore volume and initial oil in place (IOIP) values were obtained through initialization running, after which the next step could be executed (see Figure 3).

Table 1 Comparison of initialization results for simulation and physical data.

Initialization Parameter	Core ID					
	17 (KAS)	**56 (KAS)**	**67 (KAS)**	**27 (TPN)**	**56 (TPN)**	**47 (TPN)**
Simulation						
Pore volume, cc	3.0296	3.5324	3.0263	3.4264	3.1999	4.0100
IOIP, cc	1.1000	0.7001	0.9999	1.4000	0.9501	1.6978
Physical						
Pore volume, cc	3.03	3.53	3.03	3.43	3.20	4.01
IOIP, cc	1.10	0.70	1.00	1.40	0.95	1.70

Figure 3 depicts the matching procedure performed during the simulation process in detail. The waterflood matching process should be conducted prior to the surfactant flooding. Due to various properties of the core samples and limited relative permeability data, minor alterations of water and oil relative permeability end-point values are allowed without ignoring residual saturation values of each core. At high N_C condition, uncertain parameters are mainly focused on rock-fluid interactions, i.e. residual oil saturation, end-point and curvature of oil and water relative permeability and interpolation set (*DTRAPW* and *DTRAPN*). These parameters are adjusted in such a way as to obtain the exact response during surfactant-polymer injection.

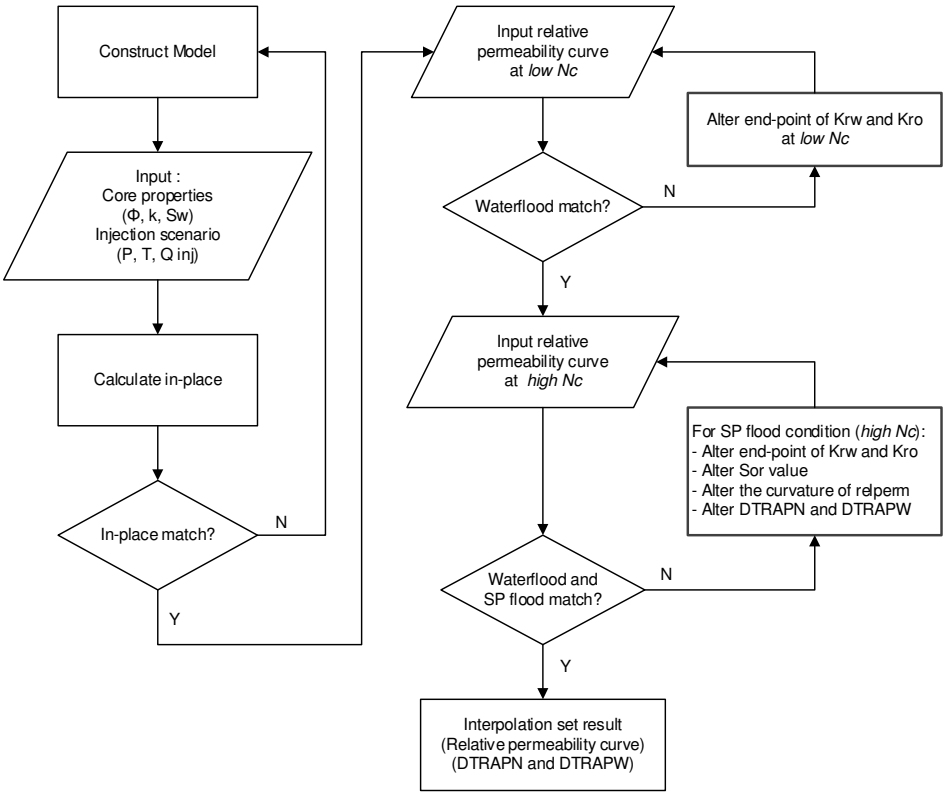

Figure 3 Coreflood simulation modeling workflow for core scale.

3 Results and Discussion

3.1 Kenali Asam Field (KAS)

Rock Properties

Detailed properties of native core named Core ID 17, 56 and 67 are presented in Table 2. Kenali Asam is a field with light oil density 42.2 API, 0.9 cP viscosity (at T = 68 °C) and its salinity reaches 8490 ppm.

Table 2 Physical and numerical properties of Kenali Asam core.

Properties	Case		
	a	**b**	**c**
Physical			
Core type	Native	Native	Native
Core ID	17	56	67
PV surfactant-polymer	0.5	0.2	0.1
Rock type	2	2	2

Properties	Case		
	a	b	c
Porosity, %	23.70	27.50	26.40
Permeability, mD	170	182	145
Pore volume, ml	3.03	3.53	3.03
Oil saturation, %	36.3	19.8	33.0
Sw irreducible, %	63.7	80.2	67.0
Sor water flood, %	11.0	10.9	18.2
Sor SP flood, %	2.0	3.3	11.9
Numerical			
Grid I (20 grids), cm	0.1860	0.1860	0.1860
Grid J (1 grid), cm	2.2330	2.2330	2.2330
Grid thickness, cm	2.2330	2.2330	2.2330
Volume modifier	0.6891	0.6925	0.6180

Surfactant-Polymer Properties

The surfactant screened for this field was AN3NS, which hit the lowest IFT point at 0.0004119 mN/m (see Figure 4). Interfacial tension values were obtained using a spinning drop tensiometer (TX5000D) operating at 6000 RPM and at 68 °C. The rheology of the single-phase polymer was investigated using a low-viscosity rotational rheometer (Brookfield DV3T) for varying rotational speed and mass concentration, as presented in Table 3.

Table 3 Polymer rheology at various concentrations.

wt%	12 RPM	30 RPM	60 RPM
0.03	1.25	1.23	1.09
0.05	1.86	1.50	1.20
0.10	2.66	1.77	1.65

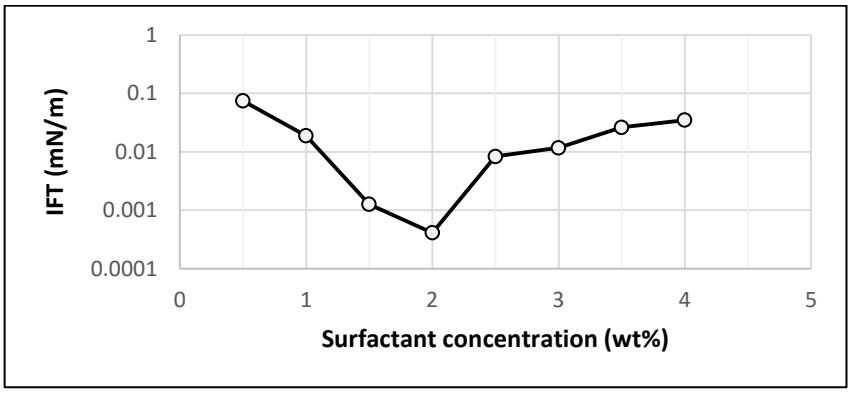

Figure 4 CMC curve of AN3NS surfactant in KAS brine.

In the numerical simulation, the 30-RPM data were selected to represent the polymer. The assumption used in this modeling was to ignore the permeability blockage and pore blockage. The measurements showed a good agreement with the research performed by Mishra for rheology observation with respect to RPM. He states that viscosity increases with increasing polymer concentrations due to the increasing intermolecular entanglement [19]. The injected concentrations are presented in weight percent, as shown in Table 4.

Table 4 Injected fluid composition in Kenali Asam coreflood simulation.

Component	Concentration (wt%)
Surfactant AN3NS	2
Polymer F3630S	0.03

The coreflood experiment deployed oil and brine sampled from layer N990 of well KAS-284, which has Rock Type 2. Rock Type 2 data were used for approximation in this study, because the relative permeability data of the well from where the core samples were taken were not available. Some data were then adjusted to the coreflood results, i.e. irreducible water and oil saturation due to water-flood and SP flood. The relative permeability profile was still kept, although the end-points were altered. This alteration was carried out using a normalization method on basic rock type data with the following formula (detailed variables information can be found under Nomenclature):

$$\frac{(x-x_{min})}{(x_{max}-x_{min})} = \frac{(y-y_{min})}{(y_{max}-y_{min})} \quad (1)$$

The alteration process was calculated until the cumulative oil profile after waterflooding matched the laboratory data. Then, the matching process was continued by matching the cumulative oil profile after SP flooding. This matching focused on the relative permeability curve as well as changes in *DTRAPW* and *DTARPN*. The literature says that at intermediate or low N_C, relative permeability for two phases will increase and residual oil saturation will decrease. The remaining oil after SP flooding can be adjusted to the experimental data either exactly or with a small deviation. The end-points of the two phases' relative permeability and curvatures can be changed arbitrarily to get a better match. This process considers the possibility of an intermediate relative permeability curve profile between before SP flooding and critical condition where it has a straight line. A straight-line profile of the relative permeability curve can be seen at ultra-low IFT (critical N_C = 2.3E−1). The laboratory experiments only gave one S_{wc} value of the oil migration process conducted during the initial experiment, where displaced water means initial oil in place. Therefore, changes in S_{wc} were not observable. The water connate

saturation can, however, be reduced at extreme condition, where all fluids in the pores are fully displaced by micellar fluid [9].

DTRAPW and *DTRAPN* are tuning parameters used to depict the alteration response to the relative permeability curve from low N_C to high N_C. These parameters can be varied after the plateau state (residual condition) of the simulation model has been matched with the laboratory data. It is paramount to check the cumulative oil profile, either steep or slant, especially in the case of SP flooding, where the slope is frequently hard to match. This shows whether the response of the oil and rock to the chemical substance is fast or not. The relative permeability at low N_C (water-flood process) had a similar profile for each of the three samples. One of them displayed an end-point of oil phase relative permeability was 2 times larger than water phase. The 2nd set of relative permeability curves had also changed into an almost straight line (ultra-low IFT condition). The interpolation parameters, i.e. *DTRAPW* and *DTRAPN*, were around −4 to −0.5. This range can be a consideration for an uncertainty analysis on field scale. 'Set 1' and 'Set 2' refer to before and after SP flooding, respectively (see Table 5).

Table 5 Interpolation parameters used in Kenali Asam coreflood simulation.

Interpolation	Core ID 17		Core ID 56		Core ID 67	
Parameter	Set 1	Set 2	Set 1	Set 2	Set 1	Set 2
DTRAPW	−6.15	−3.8	−5	−2	−5	−2.5
DTRAPN	−6.15	−0.5	−5	−4	−5	−1.5

It can clearly be seen from Figure 5 that the injected surfactant-polymer slug with a size of 0.5 PV yielded the highest oil recovery, followed by 0.2 and 0.1 PV successively. Around 40% incremental oil recovery could be achieved by injecting a mixture of 2% w/w surfactant and 0.03% w/w polymer F3630S with a slug size of 0.5 PV. Meanwhile, 0.2 PV and 0.1 PV gave around 25% and 20% of additional oil recovery, respectively. The increase in slug size gave more volume of surfactant and hence it gave more ability to penetrate deeper and alter the wettability of the rock surface. With respect to the water cut results, a decrement of up to 10% of water cut was observed soon after surfactant-polymer injection, as shown in the Appendix.

Detailed results of the coreflood matching are presented in the Appendix (Figure 10). Note that the matched relative permeability curves for waterflooing are completely different from the models used in the field-scale reservoir simulation model. Thus, conducting SCAL and updating the dynamic model is highly recommended for further full-field studies. Despite the variation in the matching results, all three investigated samples showed agreement concerning the relative permeability curves alteration. In addition, the *DTRAPW* and

DTRAPN values obtained at low N_C condition (Set 1) ranged from −5 to −6.2, as typically encountered in sandstone porous medium.

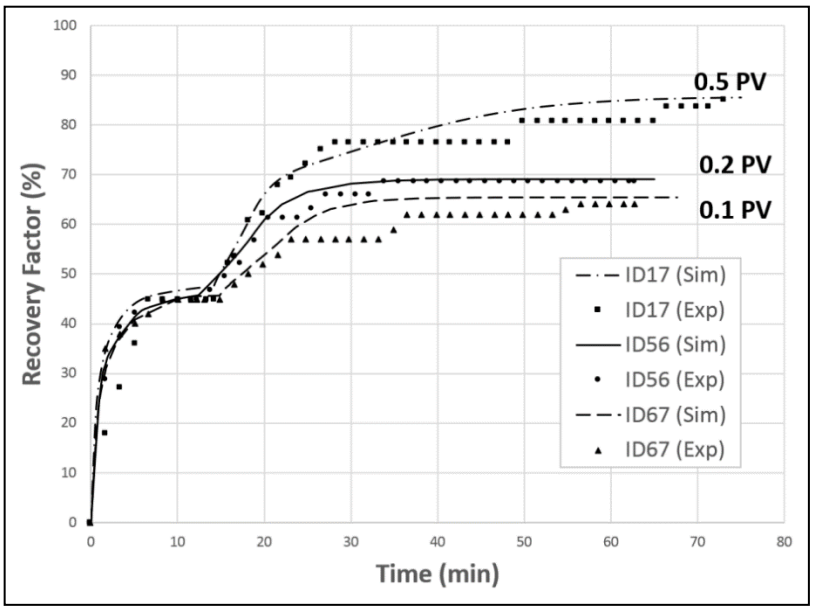

Figure 5 Oil recovery for various slug sizes of Kenali Asam cores.

The interpolation parameters acquired from the coreflood matching of Core ID 56 suggest a typical critical value of the desaturation curve encountered in the water-wet sample. As shown in Table 5, a higher value of *DTRAPN* in Set 2, from −5 to −4, indicates that the non-wetting phase, i.e. oil, experienced decreasing residual saturation more rapidly than the wetting phase. A higher value of *DTRAPN* means a higher capillary number, as illustrated in the capillary desaturation curves and the formula in literature [9].

These two interpolation parameters significantly govern the response of residual saturation reduction, which eventually affects the oil and water production increment due to surfactant injection.

3.2 Tempino Field (TPN)

Rock Properties

Table 6 displays detailed properties of the native cores called Core ID 27, 56 and 47. Tempino has 43.2 API oil density, 0.9 cP viscosity (at T = 68 °C) and a salinity of 8670 ppm. It also resumes the results of the core flood tests performed using the core flood apparatus.

Table 6 Physical and numerical properties of Tempino core.

Properties	Case		
	a	b	c
Physical			
Core type	Native	Native	Native
Core ID	27	56	47
PV surfactant-polymer	0.5	0.2	0.1
Rock type	7	7	7
Porosity, %	27.10	27.44	29.57
Permeability, mD	239	608	856
Pore volume, ml	3.43	3.20	4.01
Oil saturation, %	40.86	29.69	42.34
Sw irreducible, %	59.14	70.31	57.66
Sor water flood, %	22.47	16.25	23.16
Sor SP flood, %	13.72	13.44	20.92
Numerical			
Grid I (33 grids), cm	0.1158	0.1158	0.1158
Grid J (1 grid), cm	2.2504	2.2504	2.2504
Grid thickness, cm	2.2504	2.2504	2.2504
Volume modifier	0.6540	2.2504	1.8276

In the coreflood simulation of the Tempino field, the relative permeability of Rock Type 7 was selected, among others because the brine and oil were sampled from layer-NCE block B600 of well TPN-209. There was a normalized alteration, as performed for the Kenali Asam field, using Eq. (1). This well, T-209, is actually assigned to Rock Type 8 but has minor Rock Type 7 in nearby grids. Using Rock Type 8 gave a more unmatched history. The best approach to perform simulation was using the rock type of well TPN-217 because this well was drilled for the purpose of a coring job. The simulation file (.dat file) was restricted to well TPN-211 as the newest. This file presents the field condition as of January 1, 2014 while the coring job was carried out in the middle of 2014.

Surfactant-Polymer Properties

The surfactant screened for this field was AN2NS-M. The diluted surfactant-polymer solution gave an IFT value of 0.0022507 mN/m along with Tempino brine at a reservoir temperature of 68°C (See Figure 6). The composition of the injected fluid applied in the simulation is presented in Table 7. A comparison of the slug size effect can be seen in Figure 7.

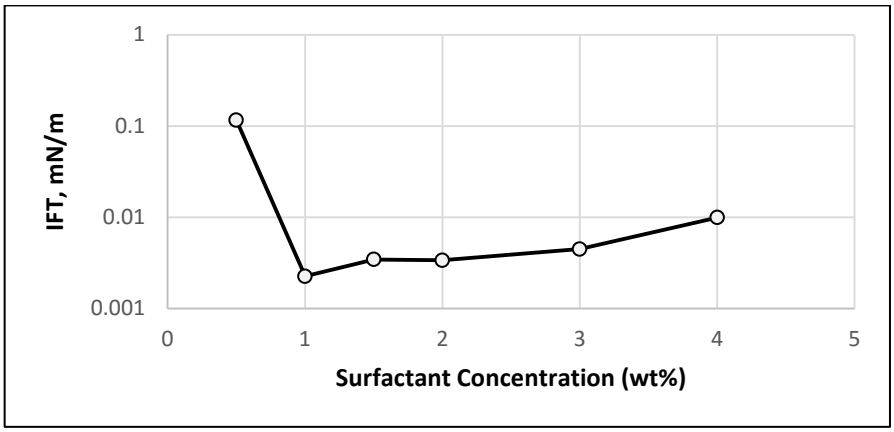

Figure 6 CMC curve of AN2NS-M surfactant in TPN brine.

Table 7 Injected fluid composition in Tempino coreflood simulation.

Component	Concentration (wt%)
Surfactant AN2NS-M	1
Polymer F3630S	0.03

The cumulative oil, the associated relative permeability curves and their alteration are presented in Appendix (Figure 11). In the Tempino coreflood simulation, only default *DTRAPW* and *DTRAPN* were employed, i.e. −5 and −2, respectively. The history-matching results for core ID 47 displayed a constant water relative permeability, while the oil relative permeability was not constant. An anomaly occurred in core ID 47, where the oil relative permeability in the 2nd interpolation set was extremely reduced, from 0.2 to 0.01. The other cores had an increased oil relative permeability in their 2nd interpolation set due to chemical injection and the default automatic simulator-generated relative permeability should be showing so. No wonder it had the smallest cumulative oil production and the slowest response after the last water injection. This uncertainty can possibly be influenced by the existence of mineral impurities that could trigger the oil bank inside the core. Hence, a separate study is currently being conducted to observe the mineral stratigraphy effect in this field. At the 19th minute, the last water flood was introduced but it only showed additional oil at the 34th minute, going from 0.77 ml to 0.78 ml. Core ID 27 gave a quick response immediately after water flooding and at the 21st minute after SP flooding. The other core, ID 56, had oil coming for additional recovery around 6 minutes after the last water flooding. Surfactant-polymer was introduced to all TPN cores at the plateau oil cumulative due to the first water flooding, obtained at the 15th, 14th and 17th minute for core ID 27, 56 and 47, respectively. While the SP flooding process was running, all cores did not give

additional oil because the chemical volume being injected was no more than 0.5 PV, hence it must still have been inside the porous medium to penetrate and flow. In this state, the chemical substance is not able to alter the rock properties yet.

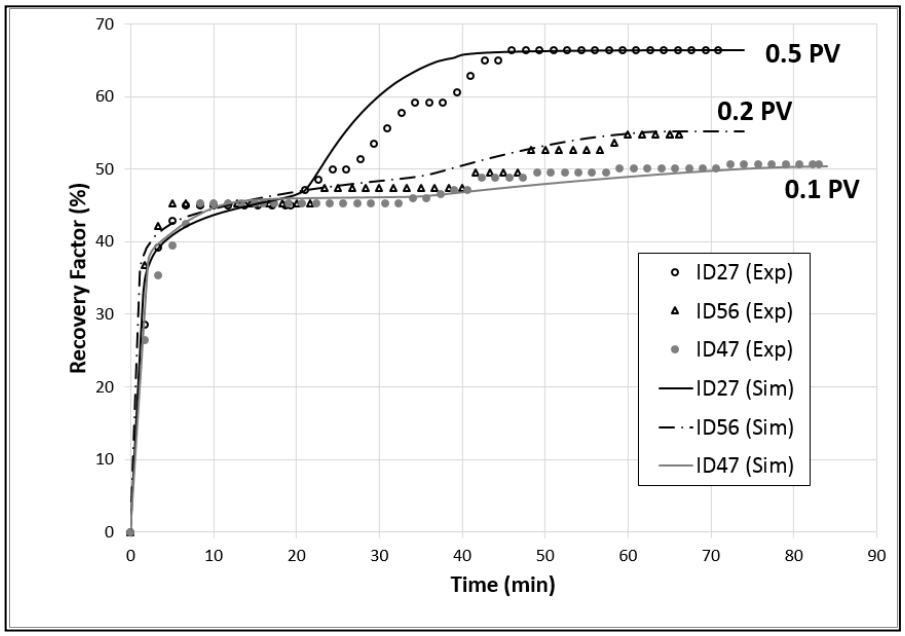

Figure 7 Oil recovery for various slug sizes in the Tempino cores.

The results in Figure 7 show the normal trend, where a larger slug size will give more oil because more surfactant-polymer is able to sweep and penetrate into a larger part of the core and for a longer time. It is crucial to consider the economical aspect, i.e. cost per barrel. This means how much money is invested for surfactant injection per recovered oil barrel.

3.3 Discussion of Interpolation Set

The experiments performed on the Kenali Asam and the Tempino fields' core samples both showed that the relative permeabilities of the investigated cores, even from the same formation, varied significantly from one core plug to another, as has been stated by Alsofi*, et al.* [21]. According to them, this is probably caused by the relatively wide changes in topology. Hence, tuning of the relative permeability is needed by assigning different residual oil saturations and connate water saturations to the normalization formula (Eq. (1)) for each core and each interpolation set (1 and 2), which describe the water flood and the surfactant-polymer flood effect, consecutively. If the alteration method is not

applied to the relative permeability prior to running the simulation of each core, the surfactant-polymer's influence may not be possible to predict. Since the authors must bring the normalized relative permeability into play, this means that the work has to be restarted with a finely detailed description of core heterogeneities, which reflects an understanding that the cores are dissimilar, even cores from the same well, and need a distinct relative permeability curve. Otherwise, whether the prediction the simulation has good agreement can only be shown by the different scenarios of varying the slug size of the injected blended surfactant-polymer. This result has pointed to some researches carried out that have reported on similar cases, in which, in order to attain a chemical EOR flooding match, the end-point of the relative permeability needed to be changed intentionally [21-23]. In this research, the authors have employed Eq. (1) rather than a well-known normalization model such as Corey's or LET's correlation, because of the absence of an attempt to determine some empirical constants. It is desirable to keep the profile of the original rock type of the field scale too.

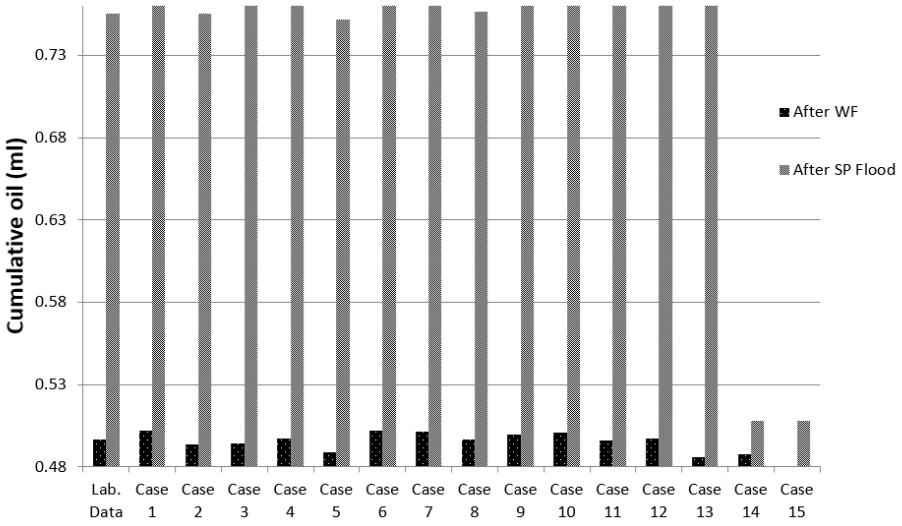

Figure 8 Sensitivity for 2nd set *DTRAPW*. Case 1 refers to the history-match case (*DTRAPW* = −3.8). The values for Cases 2 to 15 are −3.5, −3, −2.75, −2.5, −2, −1.75, −1.5, −1, −0.5, −4.3, −5, −6, −7 and −8.

A sensitivity study on the 2nd parameter set of *DTRAPW* and *DTRAPN* was conducted as well, focusing on one sample (see Figures 8 and 9). The authors selected the Kenali Asam field core ID 17 with 0.5 PV chemical injection. The core scale history match gave −3.8 and −0.5 for *DTRAPW* and *DTRAPN*, respectively; this is called 'Case 1' in Figures 8 and 9. Although the changed

variables belong to the 2nd set, the cumulative oil production during the first water-flooding process was also influenced. It is desirable that the performance is affected only after the chemical has been injected. It is what the software weakness is found.

The tested values for *DTRAPW* varied from −8 to −0.5 within a difference of 0.25 or 0.3. In the numerical simulation, the values −2.8, −4, −4.5, −4.75, −5.5, −6.5, −6.75 and −7.5 encountered a problem. An error message said that convergence was not achieved because the time step was too small. However, the same time step with another *DTRAPW* input could be executed. At particular points below the history match, the numerical performance slowed down considerably. Running the simulation took around twice as long for *DTRAPW* at −5 and −6 compared to *DTRAPW* at −3.8. No recognizable pattern resulted from either increasing or decreasing the *DTRAPW* value. Some still gave a reasonable amount of cumulative oil produced both at the end of waterflooding and SP-flooding (final simulation). However, some cases (Cases 14 and 15) were not able to give a significant cumulative oil increment (see Figure 8).

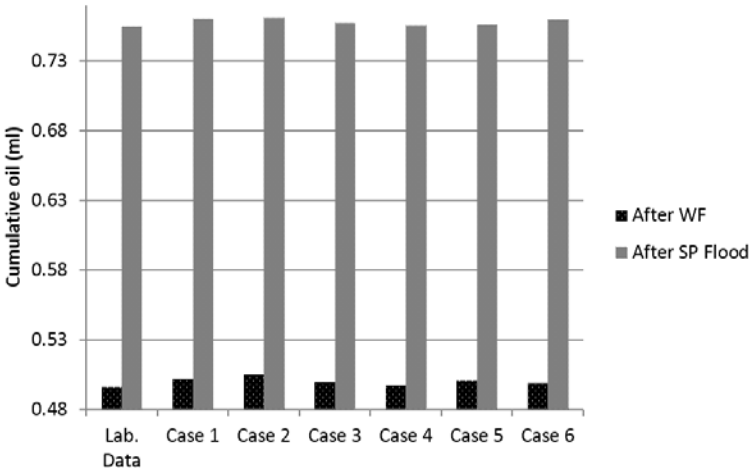

Figure 9 Sensitivity for 2nd set *DTRAPN*. Case 1 refers to the history-match case (*DTRAPN* = −0.5). The values for Cases 2 to 6 are −1, −1.3, −1.7, −2 and −2.3.

In the *DTRAPN* sensitivity study (see Figure 9), various values were applied and they still produced good results. *DTRAPN* at −2.7, −3, −3.2 and −3.8 gave a numerical error stating that convergence was not achieved. Thus, a (negative) value of either *DTRAPW* or *DTRAPN* that is too small tends to create numerical errors.

4 Conclusions

The Tempino cores appeared to be less preferentially water wet than the Kenali Asam cores, as indicated by the lower initial water saturation and higher residual oil saturation after water displacement.

The experimental results showed that displacement of residual oil by a mixture of surfactant-polymer worked better in the preferentially water wet cores. In this case, the oil recovery increment from the Kenali Asam cores (preferentially water wet) reached up to 40% after injection with the surfactant-polymer mixture slug at a size of 0.5 PV. Meanwhile, the oil recovery increment for the Tempino cores (less preferentially water wet) reached up to 21% after injection with the surfactant-polymer mixture slug at a size of 0.5 PV. In a preferentially water wet system, addition of polymer to a surfactant solution more effectively assists the lowering of the mobility ratio, hence it aids the volumetric sweep efficiency.

A combined polymer with surfactant, made of a mixture of anionic ethoxy carboxylate derived from palm oil and non-ionic ethoxylate under an appropriate composition, can reduce the IFT of a light oil-brine system at ultra-low level (around 10^{-3} to 10^{-4} mN/m), which can effectively increase oil recovery.

It has been shown that a method to change these parameters as listed below can be applied for native core of the Kenali Asam and Tempino fields. The parameters are:

1. Phase interpolation parameter (*DTRAPW* and *DTRAPN*) at low and high N_C;
2. End-point of relative permeability curve at low N_C;
3. End-point and relative permeability curve profile at high N_C; and
4. Residual oil saturation at low and high N_C.

The relative permeability curves can also be abstracted and represented from a well where oil and brine have been sampled instead of the rock-type of a cored well due to limited available information. A normalized alteration method revealed that it can be applied to gain a better history-match for waterflooding and surfactant-polymer flooding.

Acknowledgements

Our highest gratitude is presented to PT Pertamina EP for financing our research to perform a surfactant technology development study from 2012 until 2014. Thanks are also extended to all individuals associated with the project.

Nomenclature

k_{ri}	:	Relative permeability, $i = w$ (water), o (oil), g (gas), l (liquid)
N_C	:	Capillary number
$P_{cog,} P_{cow}$	:	Oil-gas capillary pressure, water-oil capillary pressure
WCRV	:	Water curvature exponent
OCRV	:	Oil curvature exponent
SCRV	:	Solution curvature exponent
GCRV	:	Gas curvature exponent
DTRAPW	:	Wetting phase interpolation set, i.e. water
DTRAPN	:	Non-wetting phase interpolation set, i.e. oil
x	:	Normalized z parameter
x_{max}	:	Maximum z parameter that follows experimental data
x_{min}	:	Minimum z parameter that follows experimental data
y	:	Original z parameter (from base rock type)
y_{max}	:	Maximum original z parameter (from base rock type)
y_{min}	:	Minimum original z parameter (from base rock type)
z	:	Parameters from water-oil table in simulator, i.e. S_w, k_{rw} and k_{ro}
S_i	:	Fluid saturation, $i = w$ (water), o (oil), g (gas), l (liquid)

References

[1] Al-Adasani, A & Bai, B., *Recent Developments and Updated Screening Criteria of Enhanced Oil Recovery Techniques*, Paper SPE-130726-MS. Presented at International Oil and Gas Conference and Exhibition in China, 8-10 June, 2010, Beijing, China. DOI:10.2118/130726-MS

[2] Austad, T., Fjelde, I., Veggeland K. & Taugbøl K., *Physicochemical Principles of Low Tension Polymer Flood*, J Petrol Sci Eng, **10**, pp. 255–269, 1994. DOI:10.1016/0920-4105(94)90085-X

[3] Samanta, A, Ojha, K, Sarkar, A. & Mandal, A., *Surfactant and Surfactant-Polymer Flooding for Enhanced Oil Recovery*, Advances in Petroleum Exploration and Development, **2**(1), pp. 13-18, 2011. DOI: 10.3968/j.aped.1925543820110201.608

[4] Gurgel, A., Moura, A. & Dantas, C., *A Review on Chemical Flooding Methods Applied in Enhanced Oil Recovery,* Brazilian Journal of Petroleum and Gas, **2**(2), pp. 83-95, 2008.

[5] Rai, S. K., Bera, A. & Mandal, A., *Modeling of Surfactant and Surfactant-Polymer Flooding for Enhanced Oil Recovery using STARS (CMG) Software*, J Petrol. Explor. Prod. Technol., 24 February 2014. DOI: 10.1007/s13202-014-0112-3

[6] Samanta, A., Bera, A., Ojh, K. & Mandal, A., *Comparative Studies on Enhanced Oil Recovery by Alkali–Surfactant and Polymer Flooding*,

Journal of Petroleum Exploration and Production Technology, **2**(2), pp. 67-74, 2012. DOI: 10.1007/s13202-012-0021-2

[7] Moore, T.F. & Slobod, R.C., *Displacement of Oil by Water-Effect of Wettability, Rate, and Viscosity on Recovery*, Paper SPE 502-G. Presented at the SPE Annual Fall Meeting, New Orleans, 2-5 October 1955. DOI:10.2118/502-G

[8] Sheng, J.J., *Modern Chemical Enhanced Oil Recovery: Theory and Practice,* Gulf Professional Publishing, Massachusetts, 2010.

[9] Van Quy, N. & Labrid, J., *A Numerical Study of Chemical Flooding--Comparison with Experiments*, Paper SPE 10202. Presented at the 1981 SPE Annual Technical Conference and Exhibition, San Antonio, Soc. Pet. Eng. J., 1983. DOI:10.2118/10202-PA

[10] Shen, P., Zhu, B., Li, X. & Wu, Y., *The Influence of Interfacial Tension on Water/Oil Two-Phase Relative Permeability*, PaperSPE-95405-MS. Presented at the 2006 SPE/DOE Symposium on Improved Oil Recovery, Tulsa, 22-26 April 2006. DOI:10.2118/95405-MS

[11] Lawson, R.G. & Hirasaki, G.J., *Analysis of The Physical Mechanisms in Surfactant Flooding*, Paper SPE-6003. Presented at the SPE-AIME 51st Annual Fall Technical Conference and Exhibition, New Orleans, Soc. Pet. Eng. J., pp. 3-6, 1983. DOI:10.2118/6003-PA

[12] Asar, H. & Handy, L.L., *Influence of Interfacial Tension on Gas-Oil Relative Permeability in a Gas-Condensate System*. SPE Reservoir Engineering, 1988. DOI:10.2118/11740-PA

[13] Regina, A., *Rate Optimization of Surfactant Flooding for 5-Spot Pattern in Tempino Field,* MSc Thesis. Petroleum Engineering Study Program, Institut Teknologi Bandung, Bandung, Indonesia, 2014.

[14] Maharsi, D.A., *Optimisation of Surfactant-Polymer Injection in Kenali Asam Field Using 5-Spot Injection Pattern*. MSc Thesis. Petroleum Engineering Study Program, Institut Teknologi Bandung, Bandung, Indonesia, 2015.

[15] Pope, G.A., Wu, W., Narayanaswamy, G., Delshad, M., Sharma, M.M. & Wang, P., *Modeling Relative Permeability Effects in Gas-Condensate Reservoirs With a New Trapping Model*, Paper SPE 62497-PA. SPE Journal, 2000. DOI:10.2118/62497-PA

[16] John, A., Han, C., Delshad, M., Pope, G.A. & Sepehrnoori, K., *A New Generation Chemical Flooding Simulator*, Paper SPE 89436.Presented atthe SPE/DOE 14th Symposium on Improved Oil Recovery, Tulsa, OK, 17-21 April, 2014.DOI:10.2118/89436-MS

[17] Patacchini, L., De Loubens, R. & Moncorge, A., *Four-Fluid-Phase, Fully Implicit Simulation of Surfactant Flooding*, Paper SPE 161630. Presented at the Abu Dhabi International Petroleum Exhibition & Conference, Abu Dhabi, UAE, 11-14 November 2012. DOI:10.2118/161630-MS

[18] Computer Modelling Group Ltd. STARS, 13 User's Guide. Calgary, Canada, 2009.
[19] Mishra, S., Bera, A. & Mandal, A., *Effect of Polymer Adsorption on Permeability Reduction in Enhanced Oil Recovery*, Journal of Petroleum Engineering **2014**, pp.1-9, 2014. DOI: 10.1155/2014/395857
[20] Swadesi, B., Marhaendrajana, T., Siregar, S. & Mucharam, L., *The Effect of Surfactant Characteristics on IFT to Improve Oil Recovery in Tempino Light Oil Field Indonesia*, J. Eng. Technol. Sci., **47** (3) pp. 250-265, 2015. DOI: 10.5614/j.eng.technol.sci.2015.47.3.2
[21] Alsofi, A.M., Liu, J.S. & Han, M., *Numerical Simulation of Surfactant-Polymer Coreflooding Experiments for Carbonates*, J. Pet. Sci. Eng., **111**, pp. 184-196, 2013. DOI: 10.1016/j.petrol.2013.09.009
[22] Hernandez, C., Chacon, L.J., Anselmi, L., Baldonedo, A., Qi, J., Dowling, P.C. & Pitts, M.J., *ASP System Design for an Offshore Application in La Salina Field, Lake Maracaibo,* SPE Reserv. Eval. Eng. **6** (3), pp. 147-156, 2003. DOI: 10.2118/84775-PA
[23] Huh, C. & Pope, G.A., *Residual Oil Saturation from Polymer Floods: Laboratory Measurements and Theoretical Interpretation,* Paper SPE 113417MS. Presented at the SPE/DOE Symposium on Improved Oil Recovery, Tulsa, OK, 19-23 April 2008. DOI: 10.2118/113417-MS

Appendix

Relative Permeability and Capillary Pressure Interpolation Formula [13,14,18]

$$\begin{aligned} k_{rw} &= k_{rwA} \times (1 - wtr) + k_{rwB} \times wtr \\ k_{ro} &= k_{roA} \times (1 - oil) + k_{roB} \times oil \\ k_{rg} &= k_{rgA} \times (1 - gas) + k_{rgB} \times gas \\ P_{cog} &= P_{cogA} \times (1 - pcg) + P_{cogB} \times pcg \\ P_{cow} &= P_{cowA} \times (1 - pcw) + P_{cowB} \times pcw \end{aligned} \tag{2}$$

where

$$\begin{aligned} wtr &= ratw^{WCRV} \\ oil &= ratn^{OCRV} \\ gos &= ratw^{SCRV} \\ gas &= ratn^{GCRV} \\ pcw &= \frac{wtr + oil}{2} \\ pcg &= gas \end{aligned} \tag{3}$$

$$ratw = \frac{log_{10}(N_c) - DTRAPWA}{DTRAPWB - DTRAPWA} \tag{4}$$

$$ratn = \frac{log_{10}(N_c) - DTRAPNA}{DTRAPNB - DTRAPNA}$$

Selected Coreflood Matching Results of KAS and TPN Core

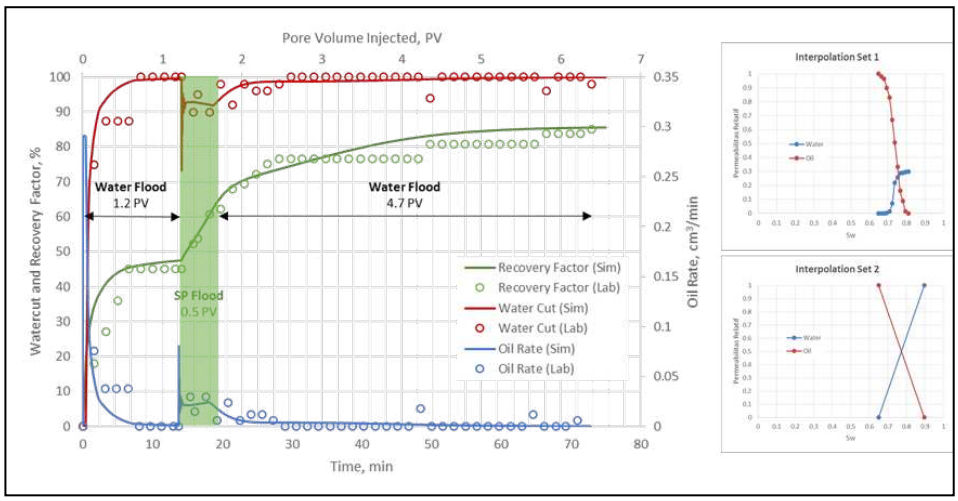

Figure 10 KAS coreflood simulation (core ID 17) with slug size 0.5 PV. The right part shows the change of relative permeability of Set 1 (waterflooding) into Set 2 (SP flooding).

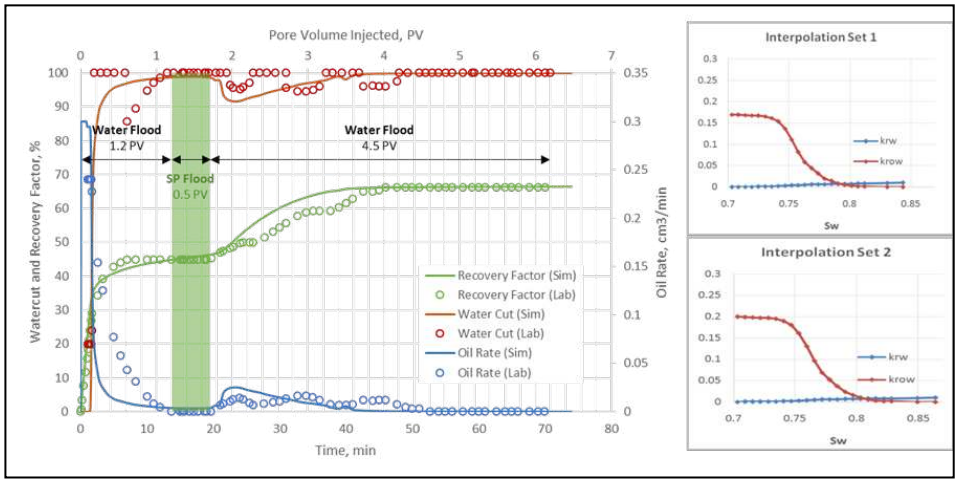

Figure 11 TPN coreflood simulation (core ID 27) with slug size 0.5 PV. The right part shows the change of relative permeability of Set 1 (waterflooding) into Set 2 (SP flooding).